DOI: 10.1534/genetics.109.111393

FRQ-Interacting RNA Helicase Mediates Negative and Positive Feedback in the Neurospora Circadian Clock

Mi Shi,*,[1] Michael Collett,*,[2] Jennifer J. Loros*,† and Jay C. Dunlap*,[3]

*Departments of *Genetics and †Biochemistry, Dartmouth Medical School, Hanover, New Hampshire 03755*

Manuscript received October 27, 2009
Accepted for publication November 25, 2009

ABSTRACT

The Neurospora circadian oscillator comprises FREQUENCY (FRQ) and its transcription activator, the White Collar Complex (WCC). Repression of WCC's transcriptional activity by FRQ via negative feedback is indispensable for clock function. An unbiased genetic screen that targeted mutants with defects in negative feedback regulation yielded a fully viable arrhythmic strain bearing a novel allele of *FRQ-interacting RNA helicase* (*frh*), an essential gene that encodes a putative exosome component protein. In the allele, frh^{R806H}, clock function is completely disturbed, while roles of FRQ-interacting RNA helicase (FRH) essential for viability are left intact. FRH^{R806H} still interacts with FRQ, but interaction between the FRQ–FRH^{R806H} complex (FFC) and WCC is severely affected. Phosphorylation of WC-1 is reduced in the mutant leading to constantly elevated WCC activity, which breaks the negative feedback loop. WCC levels are considerably reduced in the mutant, especially those of WC-1, consistent both with loss of positive feedback (FRQ-dependent WC-1 stabilization) and with a reduced level of the FRQ-mediated WCC phosphorylation that leads to high WCC activity accompanied by rapid transcription-associated turnover. FRH overexpression promotes WC-1 accumulation, confirming that FRH together with FRQ plays a role in WC-1 stabilization. Identification of a viable allele of *frh*, displaying virtually complete loss of both negative and positive circadian feedback, positions FRH as a core component of the central oscillator that is permissive for rhythmicity but appears not to modulate periodicity. Moreover, the results suggest that there are clock-specific roles for FRH that are distinct from the predicted essential exosome-associated functions for the protein.

CIRCADIAN clocks are an evolutionarily conserved means through which metabolic, physiological, and developmental processes are controlled (Bell-Pedersen *et al.* 2005; Gatfield and Schibler 2007; Brunner and Kaldi 2008). A circa 24-hr clock allows organisms to predict day–night changes thus providing them benefits for survival (Ouyang *et al.* 1998; Dodd *et al.* 2005). Our understanding of the circadian clock has advanced dramatically since clock genes *period* and *frq* were cloned in Drosophila and Neurospora, respectively (Young and Kay 2001; Dunlap 2008). Since then, research on many model organisms has revealed a conserved aspect of regulation in which negative feedback plays an essential role in maintaining a self-sustained circadian clock (Dunlap 1999; Heintzen and Liu 2007; Mackey 2007). The circadian oscillator in fungi and animals, for instance, comprises a negative element(s) whose gene product(s) inhibits the activity of its own transcriptional activators (positive elements), a heterodimer of proteins interacting via PAS domains (Young and Kay 2001). The inhibition combined with delayed turnover of the negative elements leads to oscillatory transcription factor activity. Since those positive elements also control expression of other genes (named *clock-controlled genes*, *ccgs*), the negative feedback loop gives rise to rhythmic expression of many *ccgs* that are involved in processes of metabolism, development, stress responses, etc.

In the Neurospora clock, components of the FREQUENCY (FRQ)–White Collar Complex (WCC)-based oscillator have been identified by forward genetics, and negative feedback was proven by showing that FRQ overexpression would stop the clock (McClung *et al.* 1989; Aronson *et al.* 1994). Subsequent identification of the heteromeric WCC as the activator of *frq* expression provided the minimal set of elements for the feedback loop, and the model of the core oscillator as a single negative feedback loop (Crosthwaite *et al.* 1997). Later work established that FRQ actually binds to and inhibits the activity of its own transcription activators, the WCC (Cheng *et al.* 2001a; Denault *et al.* 2001; Froehlich *et al.* 2003), and this negative feedback gives rise to rhythmic expression of *frq* and other *ccgs* (Correa *et al.* 2003). In the current view of the feedback loop, newly synthesized FRQ enters the

Supporting information is available online at http://www.genetics.org/cgi/content/full/genetics.109.111393/DC1.

[1]*Present address:* Department of Neuroscience, Howard Hughes Medical Institution, University of Pennsylvania, Philadelphia, PA 19104.

[2]*Present address:* Fonterra Research Centre, Private Bag 11029, Palmerston North 4442, New Zealand.

[3]*Corresponding author:* 7400 Remsen, Department of Genetics, Dartmouth Medical School, Hanover, NH 03755.
E-mail: Jay.C.Dunlap@dartmouth.edu

nucleus, where it brings casein kinase (CK I) and CK II to phosphorylate the WCC and inhibits its activity (Schafmeier *et al.* 2005; He *et al.* 2006). In the process, appreciable levels of the FRQ–WCC complex are seen in the nucleus, and the feedback loop is finally closed as FRQ-mediated phosphorylation of the WCC impedes DNA binding, WCC is stabilized (Schafmeier *et al.* 2008), and the complex is exported from the nucleus (Hong *et al.* 2008).

An important addition to the understanding of the cycle came when a putative RNA helicase found to copurify with FRQ was shown to be essential for the clock (Cheng *et al.* 2005). The FRQ-interacting RNA helicase (FRH), encoded by an essential gene, *frh*, shows significant homology to mtr4p, a cofactor of the Saccharomyces exosome complex involved in mRNA export and degradation (Mitchell and Tollervey 2000). Recently it was shown that FRH interacts, albeit weakly, with exosome components and strains with reduced FRH have reduced *frq* mRNA stability (Guo *et al.* 2009).

To further understand the mechanism of negative feedback, we utilized a genetic screen aimed at uncovering components required for feedback. A strain, Mut10, was isolated, which showed essentially normal growth and viability but an arrhythmic phenotype. Genetic mapping revealed a chromosomal translocation in the strain tightly linked to a missense mutation (R806H) in the *frh* locus. Those two mutations were separated and the clock phenotype was shown to be due to the R806H change in FRH, which leads to a weakened interaction between FRQ and the WCC and a defect in WCC phosphorylation. While confirming involvement of FRH in negative feedback, this result strongly suggests that the essential functions of FRH do not constitute important elements of the clock cycle, since the *frh* mutant strain shows normal growth and development while having completely lost circadian regulation. Interestingly, WC-1 and WC-2 are both downregulated in the mutant strain, suggesting that FRH, like FRQ, participates in the interlocked positive feedback loop that maintains WCC stability (Lee *et al.* 2000; Cheng *et al.* 2001b; Schafmeier *et al.* 2006, 2008).

MATERIALS AND METHODS

Plasmids, strains, media, and Neurospora methods: All strains used in this research included in their genetic background the *ras-1^{bd}* allele that serves to clarify the clock-controlled conidiation pattern in race tube assays (Belden *et al.* 2007). Because *ras-1^{bd}* does not affect the rhythm but only clarifies its expression, strains bearing only *ras-1^{bd}* are referred to here as "wild type" (WT). A construct pYL51A was made by Y. Liu, containing the *hph* gene with *frq* 3′-UTR under control of the *frq* promoter and the *frq* ORF under control of the *qa-2* promoter. pYL51A was targeted to the *his-3* locus and the strain containing the reporter gene, 197-9 [*ras-1^{bd}, his-3::(frqp-hph-frq3′ UTR, qa-2p-frq)*], was subjected to EMS mutagenesis as described below. The knock-in (KI) constructs *frh$^{R806H\text{-}KI}$*, *qa-frh*, *qa-wc-1*, and *qa-wc-2* were transformed into the *ras-1^{bd}; mus-52* strain to avoid ectopic integration via nonhomologous recombination (Ninomiya *et al.* 2004; Colot *et al.* 2006). The transformants were backcrossed to WT to obtain homokaryon knock-in strains.

Media recipes and Neurospora manipulation methods are adapted from those available at the Fugal Genetics Stock Center (FGSC) (http://www.fgsc.net/Neurospora/NeurosporaProtocolGuide.htm and http://www.fgsc.net/methods/stanford.html). The race tube assay has been described elsewhere (Aronson *et al.* 1994). The race tube medium contained 1× Vogel's salts, 0.1% glucose, 0.17% arginine, 50 ng/ml biotin, and 1.5% Bacto-agar. The regular liquid culture medium contained 1× Vogel's salts, 2% glucose, 0.5% arginine, and 100 ng/ml biotin. The quinic acid (QA) induction liquid culture medium contained 1× Vogel's salts, 0.1% glucose, 0.5% arginine, 100 ng/ml biotin, and 0.01 m QA. Race tubes were analyzed as previously described (Shi *et al.* 2007).

Genetic screen for negative feedback loss mutants: A liquid suspension of conidia from strain 197-9 (2×10^7/ml) was treated with 100 mm EMS in 0.067 m potassium phosphate buffer (pH 7.0) for 5 hr. The treated conidia, which displayed an ~25% survival rate, were washed three times with buffer and diluted 10-fold in the final wash. Conidial suspension (~10^7 cells) was plated onto 1× Vogel's plus 1× FIGS plates with 400 μg/ml hygromycin. The plates were cultured in constant dark and in total, 83 surviving colonies were picked after 7 days of culture.

DNA and RNA analyses: Neurospora genomic DNA was prepared from liquid cultures using the Puregene DNA isolation kit from Gentra Systems. Neurospora RNA was prepared as previously described (Aronson *et al.* 1994). In Southern analysis, 0.5 μg restriction digested genomic DNA was resolved on a 1% agarose gel and the digoxigenin (DIG) system from Roche was used for probe labeling and detection. In Northern analysis, 10 μg total RNA was resolved on a 1.2% agarose gel containing 2% formaldehyde, and the DIG system was used for probing and detection. Allele-specific PCR was used to differentiate SNP genotypes of mapping progeny or *frh* alleles of mutant and knock-in strains. Allele specific DNA oligos were designed with the online SNAPER program (http://ausubellab.mgh.harvard.edu/). Oligo MS266 (AAGC CATTGTTATCGCCGTTGA) and MS254 (GAACGATGTTC GGCTGTAGGTA) flanked the translocation site and the PCR product was used in Southern analysis for chromosomal translocation.

Antiserum generation and protein analysis: FRQ, WC-1, and WC-2 antibodies have been described (Garceau *et al.* 1997; Lee *et al.* 2000; Denault *et al.* 2001). Preparation of FRH antibody was adapted from Cheng *et al.* (2005). Western analysis, immunoprecipitation, and phosphatase treatment were performed as previously described (Garceau *et al.* 1997).

SNP marker identification and SNP mapping: Conidia of a *Mauriceville* isolate (FGSC no. 2225) were cultured at 30° in constant light (LL) for 4 hr. A cDNA library was made from the extracted mRNA using a Stratagene Uni-Zap kit. The cDNA clones were sequenced and SNP markers were identified by comparing the *Mauriceville* sequences with the genomic sequence of the reference *Oak Ridge* isolate (Lambreghts *et al.* 2009). SNP6 and SNP72 on LGI were named after the contig numbers where they are localized (http://www.broad.mit.edu/annotation/genome/neurospora/Home.html) and selected for mapping purposes. Additional SNP markers between those two markers were found by sequencing part of the *Mauriceville* genomic DNA in this region. Progeny from a cross between WT in *Mauriceville* and Mut10 in *Oak Ridge* were subject to SNP mapping. The rhythmicity phenotype was scored using the race tube assay and the SNP genotype was scored by allele-specific PCR.

Sequence analysis of the chromosome translocation: *Kpn*I digests of Mut10 genomic DNA were self-ligated and subjected to inverse PCR with DNA oligos near the mapping locus on LGI. The PCR products were cloned and sequenced to obtain the region of chromosome translocation.

Forced heterokaryon assay: Mut10 was individually crossed with *inl* and *pan-2*. Progeny were screened for Mut10; *inl* and Mut10; *pan-2* strains. A forced heterokaryon strain of Mut10 and WT was obtained by culturing Mut10; *inl* and *pan-2* together on minimal medium, as well as the reciprocal heterokaryon of Mut10; *pan-2* and *inl*.

Real-time PCR analyses: cDNA samples were prepared with the Invitrogen Superscript III RT reaction kit. Real-time PCR analyses were performed using the power SYBR Green system from ABI.

RESULTS

A novel genetic screen for negative feedback mutants: The concept underlying circadian negative feedback is that the protein product of the *frq* locus acts to turn down its own expression. Therefore, to develop a screen for mutations affecting negative feedback, we engineered a strain bearing (1) a selectable marker under control of the *frq* promoter, and (2) a means through which FRQ could be overexpressed. In this strain, when FRQ is overexpressed, the selectable marker should be turned off unless the feedback loop connecting FRQ to repression is blocked by mutation. Specifically, we constructed strain 197-9 [*ras-1^{bd}, his-3::(frqp-hph-frq3′ UTR, qa-2p-frq)*], which contains (1) the selectable marker gene *hph* under control of the *frq* promoter and thereby activated by the transcription factor WCC and (2) the *frq* ORF under control of the QA inducible *qa-2* promoter (Figure 1A). Expression of *hph* encodes hygromycin phosphotransferase, which confers cell resistance to hygromycin. Since FRQ represses WCC activity in constant darkness (DD), growth of the strain was inhibited in darkness under hygromycin selection. However, since *frq* is expressed in the light regardless of the degree of FRQ overexpression (Crosthwaite *et al.* 1995), the strain was hyg resistant in the light. After EMS mutagenesis, survivors were plated and kept in the dark under hygromycin, which killed most of cells. Out of ~10^7 mutated conidia, 83 mutants grew on hygromycin, therefore signaling a potential loss of negative feedback. Among those mutant strains, 21 were arrhythmic, 6 showed period lengths longer than WT, and 13 showed shorter period lengths, and the remaining mutants showed no obvious defects in clock oscillation, suggesting that they developed alternative means of resistance. These data are consistent with the concept that negative feedback is essential for the circadian clock and that defects in this regulation might lead to clock phenotypes.

Since FRQ is a negative element in the oscillator (Aronson *et al.* 1994), we assumed that some mutants represented *frq* alleles. To identify the *frq* mutants, arrhythmic strains were crossed with 732-1 (*frq^7, un-10; ras-1^{bd}; a*). The *frq^7* allele confers a long period length (~29 hr) and *un-10*, which is tightly linked to *frq*, is temperature sensitive for growth. So in these crosses, novel alleles of *frq* arising from the EMS mutagenesis and screen would fail to segregate progeny with wild-type rhythms and virtually all *un-10* strains would have a 29-hr period length. In this way, 6 of the 21 arrhythmic mutants were localized to *frq*, and the recessive nature of these mutations was confirmed by a failure to grow on

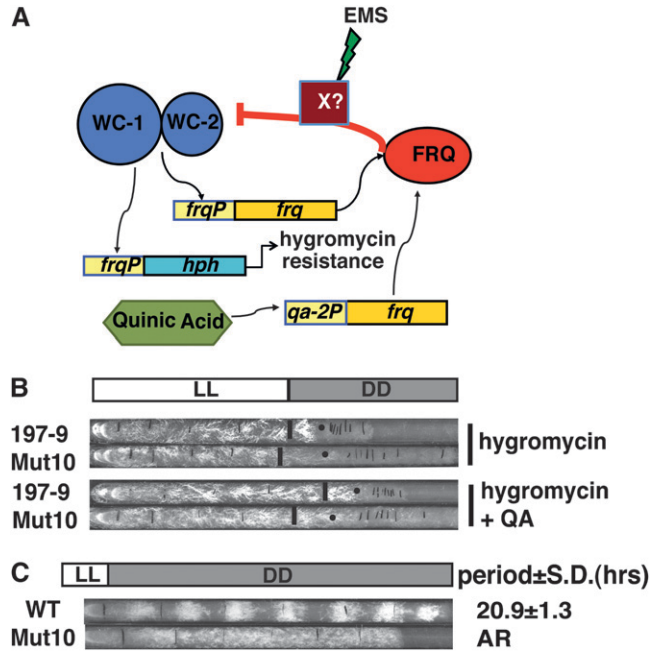

Figure 1.—A genetic screen for mutants defective in circadian negative feedback. (A) Scheme of the genetic screen. Expression of the selectable marker, *hph*, is under control of the *frq* promoter (*frq*P); therefore it is repressed by negative feedback in the dark via FRQ inhibiting the WCC transcriptional activity. Mutants with defects in negative feedback were obtained after EMS mutagenesis through selection for resistance to hygromycin. Overexpression of FRQ by QA induction driven through the *qa-2* promoter (*qa-2*P) was subsequently used to confirm that there was a break in the negative feedback loop connecting FRQ to the WCC. (B) Race tube assay with hygromycin selection. The mycelial growth front was marked with a thin black line each day. The thick solid black lines on race tubes represent light (LL) to dark (DD) transfer. The dots mark growth fronts 1 day after LD transfer. The original strain 197-9 that was subjected to EMS mutagenesis grew normally in light, reflecting light-induced WCC activity that activates the *frq*P. After LD transfer, the growth rate decreased dramatically, verifying that the WCC activity was inhibited by FRQ. In comparison with 197-9, the growth rate of Mut10 was faster in DD, suggesting that negative feedback was severely affected. Consistent with this, QA-induced FRQ could not restore the loss of negative feedback in Mut10, confirming that the strain contains a *bona fide* feedback mutation not at the *frq* locus. (C) Race tube assay in free running conditions. WT and Mut10 sibling strains were cultured in light and their clocks were assayed after transfer to DD. Mut10 is arrhythmic under free running conditions, although its growth rate is comparable to the WT sibling strain. Period length is shown from a regression analysis of $n = 6$ bands with a standard deviation (SD). AR, arrhythmic.

plates containing hygromycin and QA. These novel *frq* alleles were set aside and attention focused on the mutations identifying potential new clock genes.

A novel mutation conferring a loss of negative feedback and an arrhythmic phenotype: Among the strains corresponding to the remaining 15 arrhythmic mutants was Mut10. On race tubes with hygromycin selection, both Mut10 and the control strain (197-9) grew normally in light, confirming that WCC activity is not repressed by FRQ in light (Crosthwaite *et al.* 1995). After L-D (light to dark) transfer, growth of 197-9 dropped dramatically, reflecting the repression of WCC activity by negative feedback. In comparison, the growth rate of Mut10 slowed but then rebounded, suggesting that negative feedback is severely affected. In this strain, overexpression of FRQ by QA could not restore negative feedback, confirming that Mut10 is not a *frq* allele but a *bona fide* negative feedback mutant (Figure 1B).

The Mut10 strain is profoundly arrhythmic on race tubes under free running conditions in the dark with regular medium, suggesting that the loss of negative feedback indeed disrupts clock function (Figure 1C). While the conidiation rhythm as seen on race tubes is an output of the circadian clock, it can mask the underlying clock rhythm in certain conditions (Shi *et al.* 2007). To confirm the circadian phenotype at the molecular level, the time course of *frq* mRNA expression was followed in the mutant strain with Northern analysis. Consistent with previous reports (Aronson *et al.* 1994), *frq* mRNA in the WT strain oscillated in a circadian manner with two peaks around time points DD12 and DD36 (Figure 2A). In the Mut10 strain, overall *frq* message level was distinctly elevated compared with WT and the *frq* expression pattern showed a random fluctuation presumably reflecting the loss of negative feedback regulation (Figure 2A). As expected (Garceau *et al.* 1997), FRQ expression and protein phosphorylation oscillated in the WT strain (Figure 2B). In comparison, FRQ expression in Mut10 was constitutively high with all phospho-isoforms present at all time points (Figure 2B), as if there were overexpression of FRQ resulting from abundant *frq* transcription, but the newly synthesized FRQ could not shut down *frq* transcription effectively due to defects in negative feedback.

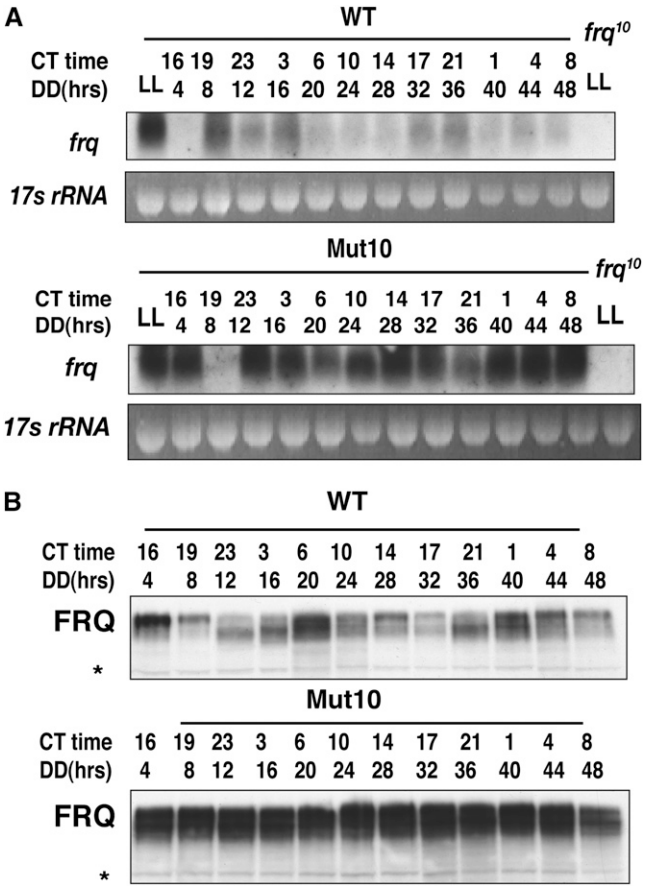

Figure 2.—Loss of negative feedback in Mut10. (A) Northern analysis showing rhythmic *frq* expression in the molecular clock. RNA samples collected over 2 days from a WT strain (top) were subjected to a Northern analysis probing with *frq*. A normal circadian *frq* mRNA oscillation was observed with two peaks around time DD12 (12-hr culture in dark) and DD36, respectively. In Mut10 (bottom), *frq* mRNA was upregulated and displayed a random fluctuation representing unregulated and noncircadian WCC activity due to the loss of negative feedback. (B) Western analysis of FRQ. Samples were collected every 4 hr from cultures held in constant darkness (DD) as in A, and subjected to Western analysis with anti-FRQ antiserum. A WT strain (top) showed a circadian oscillation of FRQ protein level and FRQ phosphorylation. In comparison, Mut10 (bottom), having lost negative feedback, showed a constitutively high level of FRQ and the presence of all phospho-isoforms at all time points. Asterisks mark a nonspecific band.

Single nucleotide polymorphism mapping of Mut10 identified a chromosomal translocation and a missense mutation in *frh*: Initial genetic mapping revealed little segregation between the arrhythmic phenotype of Mut10 and two genetic markers on linkage group I (LGI) near the centromere, *mat* (10.9 cM) and *his-3* (7.3 cM) (Figure 3A). SNP mapping (Dunlap *et al.* 2007; Lambreghts *et al.* 2009) using Mut10 (in the *Oak Ridge* background) and WT (in the *Mauriceville* geographical variant background of Neurospora) (Metzenberg *et al.* 1985) was used to achieve a finer genetic resolution. Consistent with the initial mapping data, the mutation was mapped to a region of ~5 MU between markers SNP6 and SNP72 near centromere I (CENI) (Figure 3A). Unexpectedly however, 2 of 10 recombinant progeny showed recombination with both SNP markers, suggesting either an exceptional frequency of double recombination, gene conversion, or the presence of a chromosomal rearrangement tightly linked to the mutation conferring arrhythmicity. To resolve this, additional SNP markers were identified by sequencing *Mauriceville* genomic DNA in the area between SNP6 and SNP72 and were scored among those recombinant progeny. Using these additional markers, Mut10 was mapped in a 20-kb region; the two "aberrant" progeny

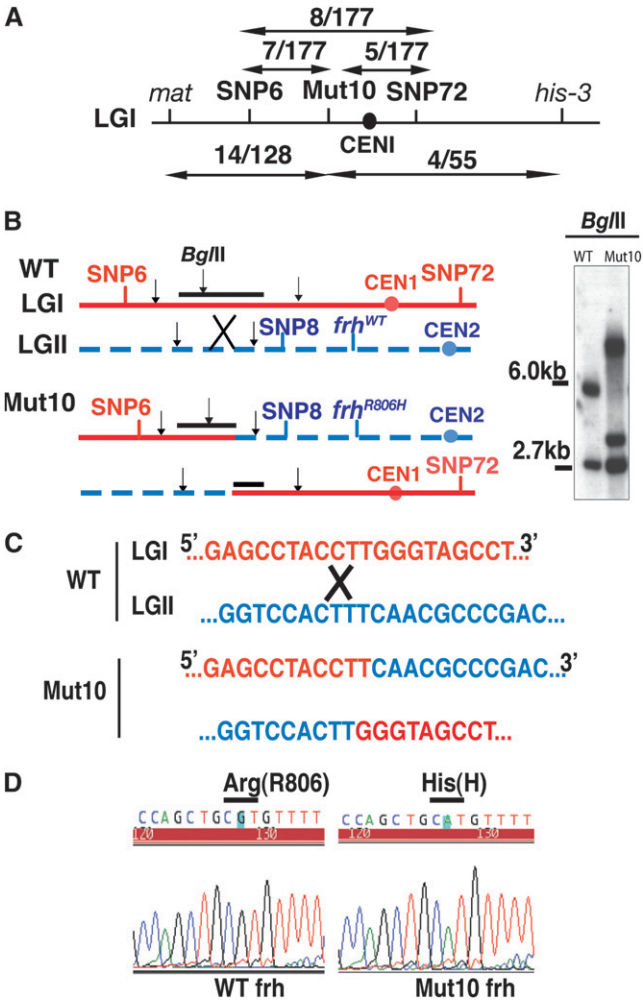

FIGURE 3.—Genetic mapping of Mut10 reveals a translocation with a breakpoint linked to *frh*. (A) Genetic mapping analyzing progeny from a cross between Mut10 and WT showed linkage to traditional markers (*mat* and *his-3)* and newly identified SNP markers near the centromere region on linkage group I (LGI). The genetic distance is reported as the number of recombinants over the number of total progeny analyzed. SNP markers were named after their contig numbers in Neurospora genome (release 7) (http://www.broad.mit.edu/annotation/genome/neurospora). (B) Chromosomal translocation in Mut10. A diagram of the chromosomes in WT and Mut10 is shown (left). The red solid line and the blue dashed line represent chromosomes of LGI and LGII, respectively, from WT (top left) and Mut10 (bottom left). The thick black bar indicates a fragment amplified by oligos MS266 and MS254 (see MATERIALS AND METHODS) from WT genomic DNA. The fragment flanks a *Bgl*II site (arrowhead) and was used as a probe in the Southern analysis (right); other *Bgl*II sites are also marked by arrows. The breakpoint of the chromosomal translocation is within the probe region, therefore the probe hybridizes to DNA from two chromosomes in Mut10, resulting in a different digestion pattern from WT as shown in the Southern analysis. See text and Figure S1 for details. (C) The translocation junction fragment was cloned by inverse PCR and sequencing of the junction region identified the exact translocation point between LGI (sequence in red) and LGII (sequence in blue). A thymidine nucleotide was lost as a result of the translocation event. (D) Sequencing of the *frh* locus in Mut10 revealed a G-to-A mutation leading to an arginine-to-histidine change (R806H).

also showed recombination with all newly identified markers, supporting the idea of a chromosomal translocation tightly associated with arrhythmicity. To confirm this and to localize the breakpoint on LGI, primer pairs were chosen in the 20-kb region from WT DNA and used for PCR using Mut10 genomic DNA as a template. All pairs except for one yielded the expected products, and the one that did not yield any product indicated the site of a chromosomal translocation breakpoint, later confirmed by Southern blot (Figure 3B).

The translocation junction fragment was cloned using self-ligation of mutant genomic DNA digest and inverse PCR. Sequencing analysis identified a reciprocal chromosomal translocation between LGI L and LGII L (Figure 3, B and C; supporting information, Figure S1 A). We hypothesized that arrhythmicity could derive from effects of the translocation on nearby gene(s), but knockouts (COLOT *et al.* 2006) of 10 ORFs on LGI near the junction showed no clock phenotype (data not shown). However, ORFs on LGII in proximity to the breakpoint included *frh* only about 100 kb away (<5 cM) from the junction site, and sequencing of Mut10 DNA identified a G-to-A transition leading to an arginine-to-histidine missense mutation as FRH^{R806H} (Figure 3D). FRH is highly homologous to mtr4p, a component of the Saccharomyces exosomal complex. The *frh* gene is essential, and even knockdowns are barely viable (CHENG *et al.* 2005), in contrast to the Mut10 strains, which are fully viable and show robust growth.

Identification of this mutation in *frh* suggested that the translocation, although tightly linked, was irrelevant to the clock defect, so SNP markers were used to score additional progeny of a Mut10 with WT cross to identify strains bearing each mutation separately (Figure S1, A and B). The strain with only the chromosomal translocation between LGI L and LGII L displayed a wild-type clock phenotype and a normal growth rate (data not shown). This strain designated as T(IL;IIL)JD10 may serve as a useful tool for genetic study in Neurospora (PERKINS 1997). FRH expression appears normal in frh^{R806H} (Figure S1 C), suggesting the mutation does not affect gene expression level or protein stability, but only the function of the protein.

Codominance of frh^{R806H} with respect to rhythm expression: Heterokaryons (HETs) were generated between Mut10 and WT strains using auxotrophic markers *pan-2* and *inl*. All heterokaryon strains show weak conidiation rhythms with approximately normal period lengths, an intermediate phenotype between Mut10 and WT (Figure 4A), indicating that frh^{R806H} is codominant to WT. Given this result, and to confirm that no additional mutations in the Mut10 background contributed to the arrhythmic phenotypes, a phenocopy approach was used. A construct bearing the frh^{R806H} fragment linked to the *bar* gene (which confers resistance to ignite) was targeted by transformation to the *frh* locus in WT (Figure S2 A). The transformants were

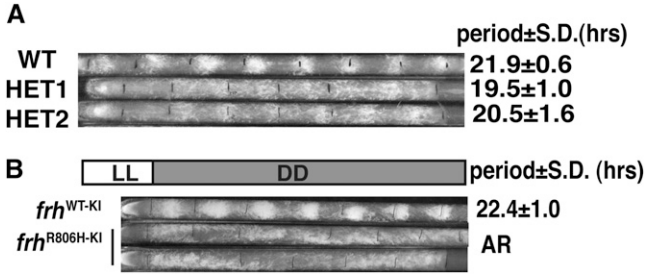

FIGURE 4.—*frh*^{R806H} knock-in phenocopies Mut10. (A) Analysis of forced heterokaryons between WT and Mut10. HET1 (heterokaryon of Mut10; *pan-2* and *inl*) and HET2 (heterokaryon of Mut10; *inl* and *pan-2*) showed weak rhythmic conidiation on race tubes with a strong conidiation background. The phenotype is between wild type and Mut10, suggesting that Mut10 is codominant with WT. Period is shown by regression analysis of $n = 6$–7 conidial bands on the race tube. (B) Race tube assay of *frh* knock-in strains (see Figure S2 for details). The *frh*$^{WT-KI}$ (SM52) strain, bearing a normal copy of *frh* with *bar* as a selectable marker, showed a normal circadian rhythm in free running conditions. In comparison, two separate *frh*$^{R806H-KI}$ strains (SM53 and SM54) showed arrhythmicity, which phenocopied Mut10 and *frh*^{R806H}.

crossed with WT to obtain homokaryotic KI progeny. Genotyping of the *frh* allele in the knock-in strains was achieved by Southern analysis and allelic-specific PCR (Figure S2, B and C). The control strain in which a WT sequence copy of *frh* linked with *bar* was knocked into the locus, *frh*$^{WT-KI}$, showed rhythmic conidiation on a race tube assay. In comparison, *frh*$^{R806H-KI}$ strains were arrhythmic (Figure 4B). These data confirm that the FRH^{R806H} missense mutation breaks the clock, probably by effectively competing with WT FRH, without adversely affecting cell viability or growth. Given the myriad essential functions of the Saccharomyces homolog of FRH, including mRNA processing, transport and stabilization, the identification of an allele that specifically abrogates the clock function without impairing essential functions is noteworthy.

Loss of positive feedback in Mut10 suggests that FRH regulates WC-1 post-translationally: As a part of the circadian negative feedback loop, FRQ inhibits DNA binding by the WCC by mediating WCC phosphorylation (FROEHLICH *et al.* 2003; SCHAFMEIER *et al.* 2005). As a result of the loss of negative feedback, WC-1 and possibly WC-2 were hypophosphorylated in Mut10 and *frh*^{R806H} strains (Figure 5, A and B and Figure S1 C). This led to an increase of WCC activity and the dramatic increase of *frq* mRNA and FRQ expression (Figure 2). Intriguingly however, WC-1 and WC-2 expression levels were very low in *frh*^{R806H}, while FRQ levels were extremely high (Figure 5 and Figure S1 C). This result seems at first paradoxical given the other role of FRQ in the post-transcriptional positive feedback loop in which, when FRQ is induced, WC-1 is upregulated within hours (LEE *et al.* 2000; CHENG *et al.* 2001b; SCHAFMEIER *et al.* 2006). The failure to induce or maintain WCC expression in *frh*^{R806H} while FRQ is overwhelmingly abundant suggested that the positive loop is disrupted in the mutant as well. To evaluate this, we examined the expression of the *wc* genes in more detail. The reduced level of WC-1 and WC-2 seen in *frh*^{R806H} could be due to reduced transcript levels and/or reduced protein stability. Transcript levels were followed by RT–PCR, revealing that both *wc-1* and *wc-2* mRNA levels were mildly reduced in *frh*^{R806H} (Figure 5C). The reduction in *wc-2* mRNA levels (approximately two- to threefold) was similar to the change in WC-2 protein and may explain the reduction in the WC-2 levels. However, the approximately twofold reduction in *wc-1* mRNA level did not seem sufficient to account for the six- to eightfold reduction in the WC-1 levels. Given this, another possibility is that FRH influences the stability of the WCC.

To assess stability, *wc-1* and *wc-2* were placed under control of the *qa-2* promoter and overexpressed in the *frh*^{R806H} background (Figure S3 A and Figure 6A). Subsequent transfer to low QA and high glucose medium repressed additional WC synthesis so WC-1 and WC-2 stability could be examined. WC-2 protein was stable in the *frh*^{R806H} background (data not shown), consistent with the possibility that downregulation of WC-2 in the mutant was at the transcriptional level. In contrast, WC-1 protein was markedly less stable in *frh*^{R806H} in comparison with *frh*^{WT}, suggesting that FRH also regulates WC-1 in a post-translational manner (Figure 6B). Recent data suggest that FRQ stabilizes WC-1 by promoting its inactivation via phosphorylation (SCHAFMEIER *et al.* 2008), and indeed Western analysis shows WC-1 to be more hypophosphorylated in the Mut10 strain (Figure 5, A and B). Since WC-1 levels are low in the mutant strains, we induced WC-1 in WT and *frh*^{R806H} respectively to compare phosphorylation (Figure 6C). WC-1 becomes hyperphosphorylated in WT apparently due to FRQ-dependent phosphorylation (SCHAFMEIER *et al.* 2005) whereas WC-1 is hypophosphorylated in *frh*^{R806H} (Figure 6C). Therefore, an interpretation consistent with the data is that FRH^{R806H} blocks or fails to promote this WC-1 phosphorylation, and the resulting hyperactive and hypophosphorylated WC-1 is unstable (SCHAFMEIER *et al.* 2008).

These results from mutant strains suggest that FRH plays its role in positive feedback through effects on WC-1 regulation. To confirm this hypothesis, we constructed *qa-frh* strains (Figure S4, A and B) in which FRH dosage is controlled by the inducer QA (ARONSON *et al.* 1994). Western analyses showed that FRH can be well induced by QA, and induction of FRH increased both FRQ and WC-1 levels (Figure 6D). All FRQ protein is bound by FRH, and FRH stabilizes FRQ (CHENG *et al.* 2005). FRH stabilizes WC-1 by promoting FRQ-dependent WC-1 phosphorylation. In summary, these results suggest that it is most likely the interaction of both FRQ and FRH as the FFC with the WCC that is essential to promote WC-1 phosphorylation and stability. In this model FRH, the

constant partner of FRQ, assists FRQ both in repressing WCC activity and in maintaining WC-1 stability, and FRH, as a component in the oscillator, has dual roles in both negative and positive feedback.

Although the level of FRQ is under circadian regulation, the amount of FRH was invariant through time (Cheng *et al.* 2005) (Figure S1 C), indicating that rhythmic production of FRH is not a part of the clock cycle. Given this, the influence of FRH dosage on period length could be assessed in a straightforward manner by using *qa-frh* strains. At low QA concentration, *qa-frh* yielded low FRH and showed a slow growth rate with arrhythmicity on race tubes. This is consistent with a previous study using RNAi to reduce *frh* expression (Cheng *et al.* 2005), and confirms that FRH plays essential roles in development and in the clock. However, the change from arrhythmicity to rhythmicity is abrupt; when FRH levels pass a certain threshold, negative feedback is recovered and the clock operates with a normal period (Figure S4 C). This result suggests that FRH functions more like a permissive "switch" for rhythmicity than a period "fine tuner."

FRH^{R806H} affects interactions among FRQ, FRH, and the WCC: FRH^{R806H} is associated with reduced WC-1 phosphorylation, and yet Q-PCR analysis confirmed that there is no difference in CKI or CKII levels between WT and *frh*^{R806H} (data not shown). Given this, two hypotheses to explain the nature of the defect in FRH^{R806H} are that the mutation might affect the interaction of FRH with FRQ or the FRH/FRQ complex with the WCC, in either case breaking the feedback loop. The first of these is not the case: Co-immunoprecipitation using α-FRH clearly showed that FRH^{R806H} still forms a complex with FRQ (Figure 7A), a finding that is consistent with codominance of the mutant. In contrast to this, the interaction between FRQ-FRH^{R806H} and the WCC is disrupted in Mut10 as indicated by reciprocal co-IP data using α-FRQ or α-WC-2 in which FRQ no longer associates with WC-2 in the Mut10 background (Figure 7B). Because a caveat of the co-IP analysis is that WCC level is low in Mut10, we

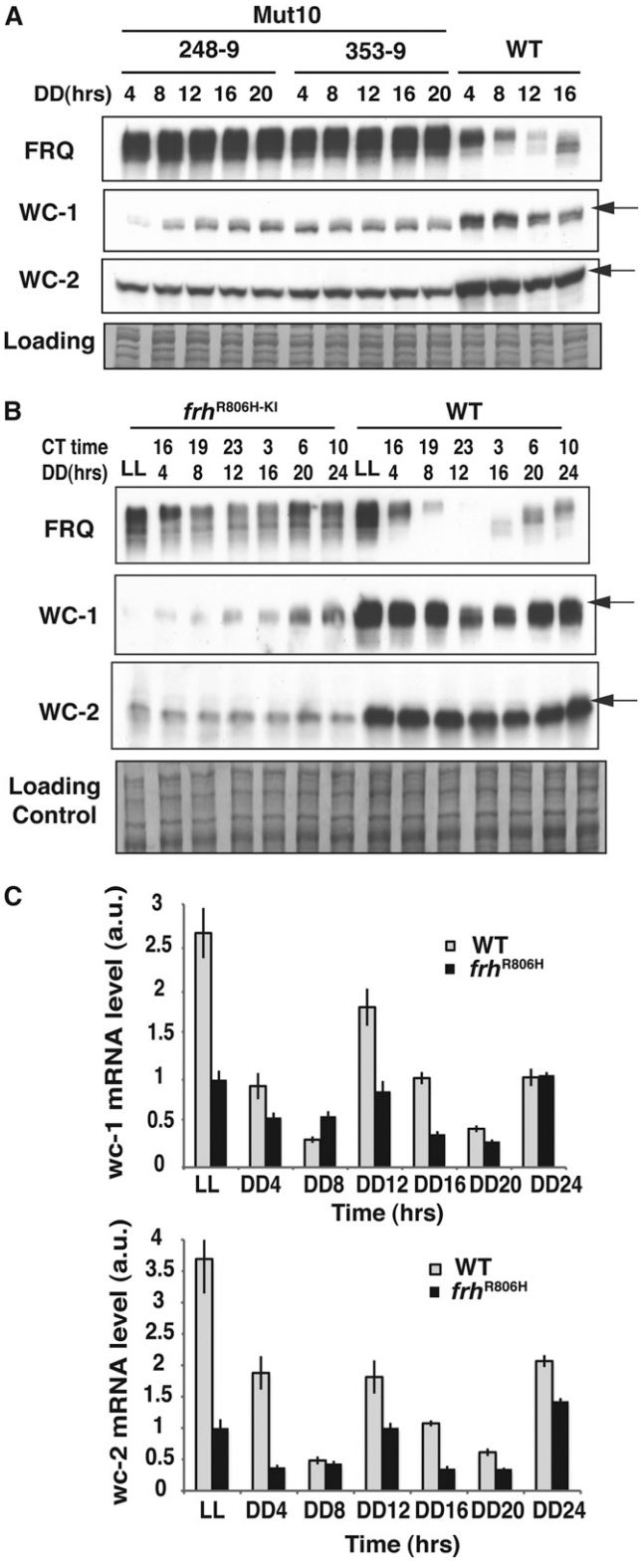

Figure 5.—Loss of positive feedback in Mut10 and *frh*^{R806H}. (A) Circadian time course samples of WT and Mut10 were subjected to Western analysis and blotted with FRQ, WC-1, and WC-2 antisera. The progeny 248-9 and 353-9 are from two successive generations of backcrosses between Mut10 and WT; both strains are arrhythmic. While FRQ levels were elevated in Mut10, WC-1 and WC-2 levels in such strains were much lower than in WT, suggesting that the high FRQ level could not maintain the WCC level, because the positive feedback loop of FRQ promoting WCC expression was disrupted in the mutant (see text for details). Arrowheads point to bands corresponding to hyperphosphorylated WC-1 or WC-2, representing inactive WCC (Schafmeier *et al.* 2005). Both White Collar proteins were hypophosphorylated in Mut10, consistent with loss of negative feedback that leads to upregulated WCC activity. (B) *frh*$^{R806H-KI}$ strains phenocopy Mut10 at the molecular level, showing defects in negative feedback leading to high expression of FRQ and defects in positive feedback leading to reduced expression of the WCC. Arrowheads point at hyperphosphorylated WCC. (C) Real-time PCR analysis of mRNA levels in samples collected over 1 day in darkness or after 24 hr in light. *wc-1* (top) and *wc-2* (bottom) mRNA levels were in general reduced in *frh*^{R806H} compared to WT. (Error bar ± SD, $n = 3$ PCR repeats.)

performed co-IP in strains in which WC-1 and WC-2 expression was driven by the *qa-2* promoter and could be artificially induced (Figure 6A). Here, despite the high level of *qa-2*-driven gene expression, the mutant strains showed low levels of WCC interacting with FRQ, especially WC-1 (Figure 7C) and were arrhythmic on race tubes (Figure S3 B). Thus, *frh*^{R806H} appears to be a clock-specific allele that affects the interaction of the FFC with the WCC, leading to a defect in the negative feedback loop.

These results, taken in the context of the forced heterokaryon data (Figure 4A), also suggest that *frq*^{R806H} acts as a dominant negative allele. We know that FRH is much more abundant than FRQ in the cell (Cheng *et al.* 2005). In heterokaryons of WT and *frh*^{R806H}, FRH^{R806H} may compete with FRH^{WT} for FRQ^{WT} interaction, partially blocking negative feedback and obscuring rhythmic conidiation on race tubes.

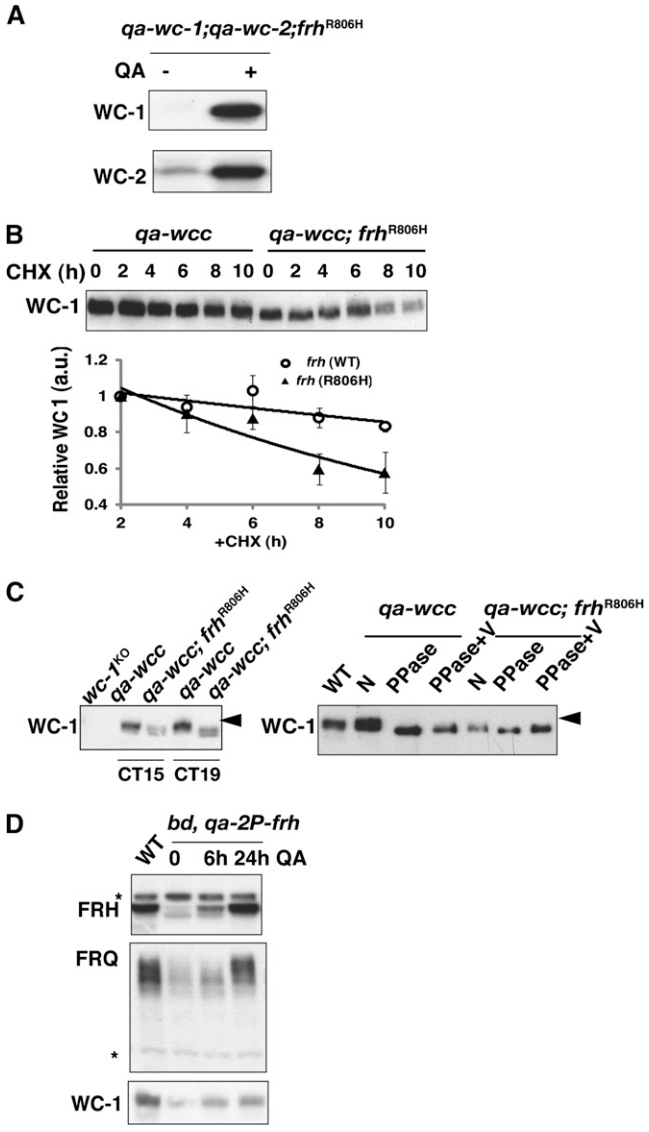

DISCUSSION

We have identified a dominant negative allele of *frh* with a discrete loss of the circadian clock-specific role(s) for the FRH protein. FRH had been previously identified as a protein copurifying with FRQ whose knockdown resulted in arrhythmicity (Cheng *et al.* 2005), and it was therefore proposed as a component of the core clock. However, because *frh* appears to be the ortholog of an essential gene in Saccharomyces, *mtr4* (*dob1*), that encodes a DEAD/DEAH box RNA helicase component of the exosome complex, and the rhythm defects were exposed only in a narrow range of expression allowing extremely weak growth and aberrant development, it was difficult to completely rule out pleiotropic effects as underlying the rhythm defect. Identification of FRH^{R806H} obviates this concern; strains bearing this mutant protein are normally robust, displaying essentially wild-type growth and development, and yet are profoundly arrhythmic. Although other explanations are possible, the simplest interpretation of the data is that all of the essential functions performed by FRH are maintained normally in FRH^{R806H}, and the corollary of this is that those essential functions may not be required for the clock-specific roles of FRH.

Figure 6.—Reduced WC-1 phosphorylation and stability in *frh*^{R806H} suggest a role for FRH in positive feedback. (A) WCC induction in *frh*^{R806H}. The *qa-wc-1; qa-wc-2; frh*^{R806H} strain was cultured in 2% glucose (−QA condition) and then moved to 0.1% glucose with 0.01 M QA (+QA condition) and grown for 8 hr. Extracts were made and subjected to Western analysis and the result showed that WC-1 and WC-2 could be induced by QA. (B) Reduced WC-1 stability in *frh*^{R806H}. WC-1 and WC-2 were induced in WT and *frh*^{R806H} by QA for 12 hr before QA was washed away and CHX was added. Time course samples collected after QA release were subjected to Western analysis and the change in WC-1 levels as determined by densitometry is plotted as a function of time. WC-1 was less stable in *frh*^{R806H} than in WT, suggesting that FRH^{R806H} had a defect in maintaining WC-1 stability and FRH has a role in post-translation regulation of WC-1. WC-2 was stable in *frh*^{R806H}. (C) Defects in WC-1 phosphorylation in *frh*^{R806H}. (Left) WCC was induced in WT and *frh*^{R806H}, and samples were cultured in dark and extracted at subjective dusk time. WC-1 in *frh*^{R806H} shows faster mobility, consistent with hypophosphorylation. (Right) WC-1 is normally phosphorylated under these conditions and can be dephosphorylated by λ-PPase and this dephosphorylation can be inhibited by sodium vanadate. Samples from CT15 (DD4) were analyzed: N signifies no addition to the reaction mix; PPase, addition of phosphatase; PPase+V, addition of both PPase and the PPase-inhibitor vanadate. (D) FRH regulates FRQ and WC-1 expression. *qa-frh*^{KI} strains were initially cultured in 2% glucose media for 48 hr (0 QA) and then moved into 0.1% glucose media with 0.01 M QA for induction. Time course samples (6 hr and 24 hr) were collected and extracts were subjected to Western analysis. FRH is inducible by QA in *qa-frh*^{KI}. Induction of FRH leads to increases in FRQ and WC-1 expression. The experiment shown is representative; variability in the kinetics of FRH, FRQ, and WC-1 induction was noted, but not in the presence of induction.

In the 1107 amino acid FRH protein, the DEAD/DEAH domain is near the N terminus, a helicase domain is in the middle of the protein, and the DSHCT (DOB1/SKY12/helY-like helicase C-terminal) domain is near to the C terminus. The R806H mutation is near to but not within the C-terminal DSHCT domain, and since all domains essential for RNA helicase function appear intact in *frh*^{R806H} which, further, does not affect the interaction with FRQ, it seems likely that this mutation is in the region specific for binding with WCC. Consistent with this, salient aspects of circadian function previously ascribed to FRQ are compromised in FRH^{R806H}. The original and principal role of FRQ in the oscillator is to mediate negative feedback: Soon after its synthesis, hypophosphorylated FRQ goes to the nucleus (Luo *et al.* 1998) and interacts with the WCC (Cheng *et al.* 2001b; Denault *et al.* 2001), resulting in a decrease in the ability of the WCC to bind to DNA (Froehlich *et al.* 2003) probably as a result of its increased phosphorylation (Schafmeier *et al.* 2005; He *et al.* 2006). FRQ then ushers the WCC out of the nucleus closing the feedback loop (Hong *et al.* 2008).

The data presented here show that FRH is clearly required for completion of the negative feedback loop because this cycle is blocked at this first step, the interaction between FRQ and the WCC, with the result that FRQ expression remains constitutively high. These data are also wholly consistent with the recent observation (Schafmeier *et al.* 2008) that transcriptionally active WC-1 is unstable and that positive feedback (Lee *et al.* 2000) is a delayed result of the FRQ-mediated WCC phosphorylation that initiates negative feedback. It is clear that FRH is also required for this, because in *frh*^{R806H}, despite the presence of elevated levels of FRQ, WC-1 and WC-2 fail to accumulate and WC-1 remains hypophosphorylated (Figure 5B). By promoting the phosphorylation of WC-1 that reduces its DNA binding and both inactivates and stabilizes it, FRH supports the positive feedback loop that allows WCC accumulation (Lee *et al.* 2000; Schafmeier *et al.* 2006). The slight decline in *wc-1* and *wc-2* mRNA levels (Figure 5C) may reflect additional subtle interconnections among the feedback loops, but because the oscillator is known to be insensitive to such changes in the levels of WCC expression (Cheng *et al.* 2001b), these minor changes in the *frh*^{R806H} strain are not likely to underlie the complete loss of rhythmicity. Rather it is the loss of

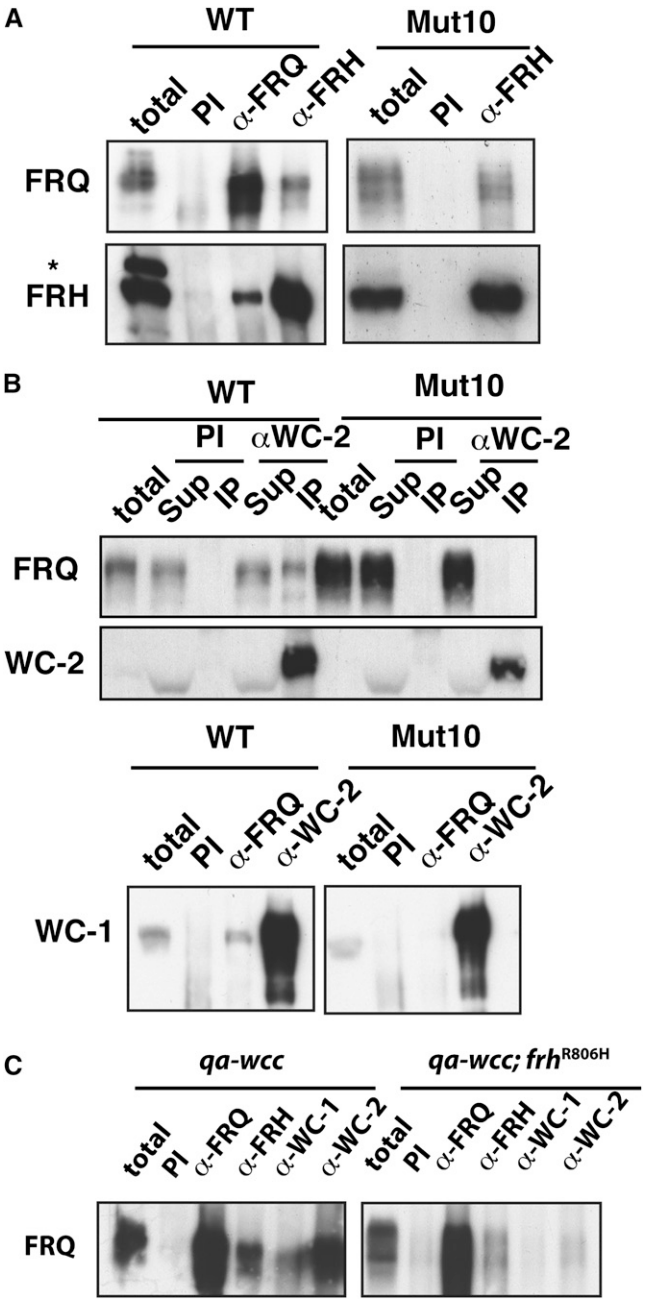

Figure 7.—The point mutation in FRH^{R806H} has no effect on FRQ and FRH interaction, but abrogates interaction between FRQ, FRH, and the White Collar Complex. (A) Co-immunoprecipitation assay. FRQ and FRH form the FRQ–FRH complex (FFC) in WT, shown by reciprocal co-IP using α-FRQ and α-FRH. Similarly, the complex formation is intact in Mut10 as well, where α-FRH co-immunoprecipitates FRQ from extracts made from Mut10 strains. PI, preimmune serum. (B) Reciprocal co-immunoprecipitation assay using α-WC-2 and α-FRQ shows that the FFC and the WCC interact in extracts from WT but not Mut10 cultures. (Top left) IP with α-WC-2 pulls down WC-2 and FRQ. (Bottom left) WC-1 is detected in the immunoprecipitates from WT extracts treated with α-FRQ or α-WC-2. In contrast, in extracts made from Mut10, α-WC-2 did not pull down FRQ (top right), neither did α-FRQ pull down WC-1 (bottom right). However in Mut10 extracts, α-WC-2 does pull down WC-1 (bottom right), indicating that the WCC is intact in Mut10. (C) Co-immunoprecipitation assay in strains where WCC is induced shows that interaction between the FRQ/FRH complex and the WCC is reduced in *frh*^{R806H}. (Left) In WT, IP with α-WC-1 or α-WC-2 pulls down FRQ. (Right) In *frh*^{R806H}, α-WC-1 or α-WC-2 pulls down some FRQ protein, but the level is reduced in comparison with WT, arguing the interaction between FFC and WCC is reduced in mutant.

negative feedback, and the data show that FRH is required with FRQ to execute this function.

A novel and potentially very powerful genetic screen for strains with defects in circadian negative feedback has also been presented, and the resolution of the defect in Mut10 presents several lessons. First it underscores the value of unbiased genetic screens, which here uncovered a very discrete mutation in an essential gene that allows a distinction to be made between the essential functions of FRH and its role as a part of the FFC in the clock. Second, the co-occurrence of the T(IL; IIL) translocation tightly linked to *frh*^{R806H} in Mut10 may serve as a cautionary note. Because the strain was fully viable and the rhythm defect was linked to the translocation that involved LGI, traditional forward genetic mapping of the arrhythmic mutant with respect to widely spaced conventional markers on LGI always failed to correctly localize *frh* on LGII. Progeny obtained by independent assortment, or through the crossover of a translocation chromosome with centromere II (bearing the mutant *frh)* and the genetically marked normal sequence chromosome bearing LGI, would be lacking all genes distal to the translocation breakpoint on LGII; these would not survive. It was only through the use of SNP markers, 6 years after the strain was isolated, that *frh*^{R806H} could be identified.

While identification of FRH^{R806H} allows separation of clock-specific functions of FRH from those functions required for cell viability, we cannot categorically exclude the possibility that some of the essential functions of FRH may also impact the clock. For example, the relatively minor downregulation of *wc-1* and *wc-2* mRNA levels in *frh*^{R806H} might signal a role for FRH in RNA stability. In any case, continued study of FRH, the FFC, and the circadian FFC–WCC complex of FRQ, FRH, WC-1, WC-2, and its associated kinases is likely to be informative.

We thank Michael Brunner and Yi Liu for feedback on the ideas prior to writing the manuscript, and Yi Liu for constructs and antisera. This work was supported by grants from the National Institutes of Health to J.C.D. (RO1 GM34985 and PO1 GM68087) and to J.J.L. and J.C.D. (RO1 GM08336).

LITERATURE CITED

Aronson, B. D., K. A. Johnson, J. J. Loros and J. C. Dunlap, 1994 Negative feedback defining a circadian clock: autoregulation of the clock gene *frequency*. Science **263:** 1578–1584.

Bell-Pedersen, D., V. M. Cassone, D. J. Earnest, S. S. Golden, P. E. Hardin *et al.*, 2005 Circadian rhythms from multiple oscillators: lessons from diverse organisms. Nat. Rev. Genet. **6:** 544–556.

Belden, W. J., L. F. Larronodo, A. C. Froehlich, M. Shi, C. H. Chen, *et al.*, 2007 The *band* mutation in *Neurospora crassa* is a dominant allele of *ras-1* implicating RAS signaling in circadian output. Genes Dev. **21:** 1494–1505.

Brunner, M., and K. Kaldi, 2008 Interlocked feedback loops of the circadian clock of *Neurospora crassa*. Mol. Microbiol. **68:** 255–262.

Cheng, P., Q. He, Q. He, L. Wang and Y. Liu, 2005 Regulation of the Neurospora circadian clock by an RNA helicase. Genes Dev. **19:** 234–241.

Cheng, P., Y. Yang, C. Heintzen and Y. Liu, 2001a Coiled-coil domain-mediated FRQ-FRQ interaction is essential for its circadian clock function in Neurospora. EMBO J. **20:** 101–108.

Cheng, P., Y. Yang and Y. Liu, 2001b Interlocked feedback loops contribute to the robustness of the Neurospora circadian clock. Proc. Natl. Acad. Sci. USA **98:** 7408–7413.

Colot, H. V., G. Park, G. E. Turner, C. Ringelberg, C. M. Crew *et al.*, 2006 A high-throughput gene knockout procedure for Neurospora reveals functions for multiple transcription factors. Proc. Natl. Acad. Sci. USA **103:** 10352–10357.

Correa, A., Z. A. Lewis, A. V. Greene, I. J. March, R. H. Gomer *et al.*, 2003 Multiple oscillators regulate circadian gene expression in Neurospora. Proc. Natl. Acad. Sci. USA **100:** 13597–13602.

Crosthwaite, S. K., J. C. Dunlap and J. J. Loros, 1997 Neurospora *wc-1* and *wc-2*: transcription, photoresponses, and the origins of circadian rhythmicity. Science **276:** 763–769.

Crosthwaite, S. K., J. J. Loros and J. C. Dunlap, 1995 Light-induced resetting of a circadian clock is mediated by a rapid increase in *frequency* transcript. Cell **81:** 1003–1012.

Denault, D. L., J. J. Loros and J. C. Dunlap, 2001 WC-2 mediates WC-1-FRQ interaction within the PAS protein-linked circadian feedback loop of Neurospora. EMBO J. **20:** 109–117.

Dodd, A. N., N. Salathia, A. Hall, E. Kevei, R. Toth *et al.*, 2005 Plant circadian clocks increase photosynthesis, growth, survival, and competitive advantage. Science **309:** 630–633.

Dunlap, J. C., 1999 Molecular bases for circadian clocks. Cell **96:** 271–290.

Dunlap, J. C., 2008 Salad days in the rhythms trade. Genetics **178:** 1–13.

Dunlap, J. C., K. A. Borkovich, M. R. Henn, G. E. Turner, M. S. Sachs *et al.*, 2007 Enabling a community to dissect an organism: overview of the Neurospora functional genomics project. Adv. Genet. **57:** 49–96.

Froehlich, A. C., J. J. Loros and J. C. Dunlap, 2003 Rhythmic binding of a WHITE COLLAR-containing complex to the *frequency* promoter is inhibited by FREQUENCY. Proc. Natl. Acad. Sci. USA **100:** 5914–5919.

Garceau, N. Y., Y. Liu, J. J. Loros and J. C. Dunlap, 1997 Alternative initiation of translation and time-specific phosphorylation yield multiple forms of the essential clock protein FREQUENCY. Cell **89:** 469–476.

Gatfield, D., and U. Schibler, 2007 Physiology. Proteasomes keep the circadian clock ticking. Science **316:** 1135–1136.

Guo, J., P. Cheng, H. Yuan and Y. Liu, 2009 The exosome regulates circadian gene expression in a posttranscriptional negative feedback loop. Cell **138:** 1236–1246.

He, Q., J. Cha, Q. He, H. C. Lee, Y. Yang *et al.*, 2006 CKI and CKII mediate the FREQUENCY-dependent phosphorylation of the WHITE COLLAR complex to close the Neurospora circadian negative feedback loop. Genes Dev. **20:** 2552–2565.

Heintzen, C., and Y. Liu, 2007 The *Neurospora crassa* circadian clock. Adv. Genet. **58:** 25–66.

Hong, C. I., P. Ruoff, J. J. Loros and J. C. Dunlap, 2008 Closing the circadian negative feedback loop: FRQ-dependent clearance of WC-1 from the nucleus. Genes Dev. **22:** 3196–3204.

Lambreghts, R., M. Shi, W. J. Belden, D. Decaprio, D. Park *et al.*, 2009 A High-Density SNP Map for *Neurospora crassa*. Genetics **181:** 767–781.

Lee, K., J. J. Loros and J. C. Dunlap, 2000 Interconnected feedback loops in the Neurospora circadian system. Science **289:** 107–110.

Luo, C., J. J. Loros and J. C. Dunlap, 1998 Nuclear localization is required for function of the essential clock protein FRQ. EMBO J. **17:** 1228–1235.

Mackey, S. R., 2007 Biological Rhythms Workshop IA: molecular basis of rhythms generation. Cold Spring Harb. Symp. Quant. Biol. **72:** 7–19.

McClung, C. R., B. A. Fox and J. C. Dunlap, 1989 The Neurospora clock gene *frequency* shares a sequence element with the Drosophila clock gene *period*. Nature **339:** 558–562.

Metzenberg, R. L., J. N. Stevens, E. U. Selker and E. Morzycka-Wroblewska, 1985 Identification and chromosomal distribution of 5S rRNA genes in *Neurospora crassa*. Proc. Natl. Acad. Sci. USA **82:** 2067–2071.

Mitchell, P., and D. Tollervey, 2000 mRNA stability in eukaryotes. Curr. Opin. Genet. Dev. **10:** 193–198.

Ninomiya, Y., K. Suzuki, C. Ishii and H. Inoue, 2004 Highly efficient gene replacements in Neurospora strains deficient for nonhomologous end-joining. Proc. Natl. Acad. Sci. USA **101:** 12248–12253.

Ouyang, Y., C. R. Andersson, T. Kondo, S. S. Golden and C. H. Johnson, 1998 Resonating circadian clocks enhance fitness in cyanobacteria. Proc. Natl. Acad. Sci. USA **95:** 8660–8664.

Perkins, D. D., 1997 Chromosome rearrangements in Neurospora and other filamentous fungi. Adv. Genet. **36:** 239–398.

Schafmeier, T., A. Haase, K. Kaldi, J. Scholz, M. Fuchs *et al.*, 2005 Transcriptional feedback of Neurospora circadian clock gene by phosphorylation-dependent inactivation of its transcription factor. Cell **122:** 235–246.

Schafmeier, T., K. Kaldi, A. Diernfellner, C. Mohr and M. Brunner, 2006 Phosphorylation-dependent maturation of Neurospora circadian clock protein from a nuclear repressor toward a cytoplasmic activator. Genes Dev. **20:** 297–306.

Schafmeier, T., A. Diernfellner, A. Schafer, O. Dintsis, A. Neiss *et al.*, 2008 Circadian activity and abundance rhythms of the Neurospora clock transcription factor WCC associated with rapid nucleo-cytoplasmic shuttling. Genes Dev. **22:** 3397–3402.

Shi, M., L. F. Larrondo, J. J. Loros and J. C. Dunlap, 2007 A developmental cycle masks output from the circadian oscillator under conditions of choline deficiency in Neurospora. Proc. Natl. Acad. Sci. USA **104:** 20102–20107.

Young, M. W., and S. A. Kay, 2001 Time zones: a comparative genetics of circadian clocks. Nat. Rev. Genet. **2:** 702–715.

Communicating editor: M. S. Sachs

GENETICS

Supporting Information
http://www.genetics.org/cgi/content/full/genetics.109.111393/DC1

FRQ-Interacting RNA Helicase Mediates Negative and Positive Feedback in the Neurospora Circadian Clock

Mi Shi, Michael Collett, Jennifer J. Loros and Jay C. Dunlap

DOI: 10.1534/genetics.109.111393

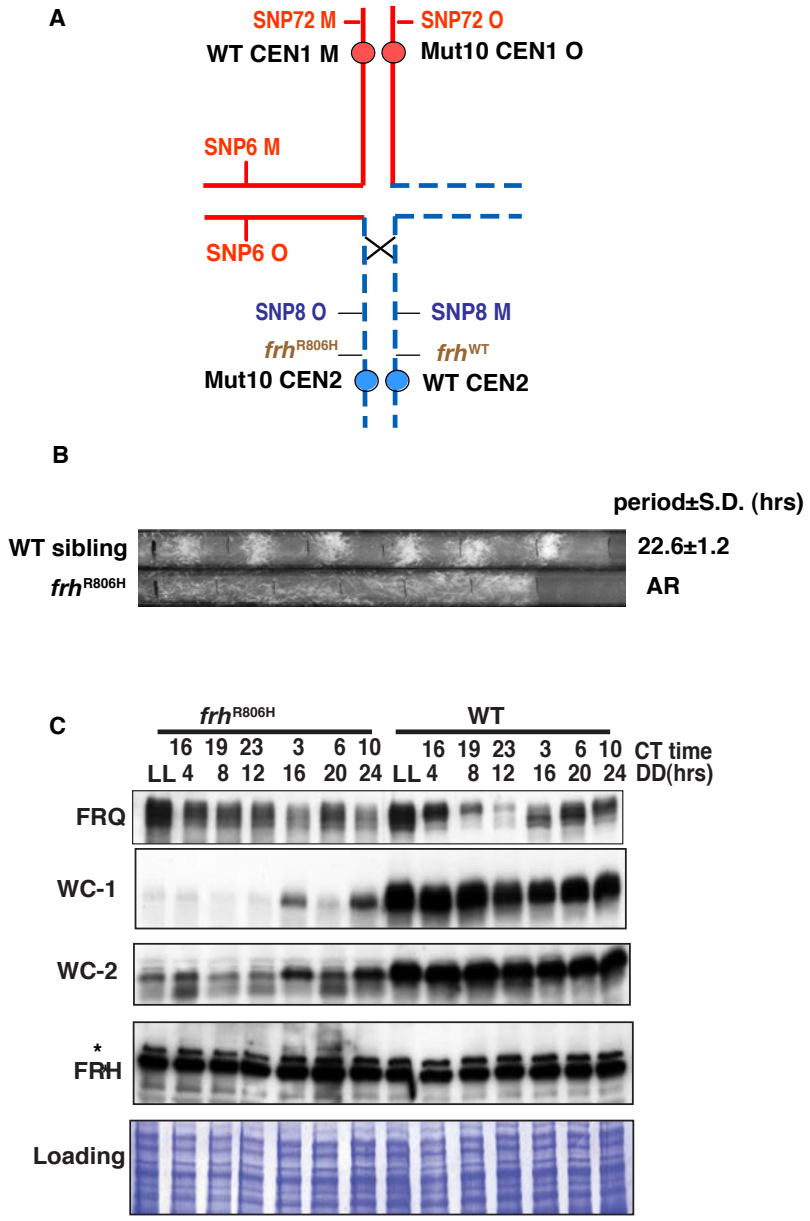

FIGURE S1.—Genetic and molecular resolution of the mutations found in the Mut10 strain. (A) Shown is an alternative view of the homology based chromosomal pairing at meiosis in a cross between Mut10 (*Oak Ridge*) and WT (*Mauriceville*). Since Mut10 contains a chromosomal translocation, pairing can only be achieved through formation of a cruciform structure during meiosis. Progeny generated from a crossover between the *frh* locus and the translocation site would separate the translocation and the *frh* missense mutation. By scoring the genetic markers shown, we obtained progeny bearing only the translocation (containing markers SNP6O and SNP72O) and progeny bearing *frh*^{R806H} but not the translocation (containing SNP6M and SNP72M). (B) Race tube assay shows that *frh*^{R806H}, like Mut10, is arrhythmic under free running conditions. (C) Western analysis of clock proteins in *frh*^{R806H} freed from the chromosomal translocation background showed elevated constitutive FRQ expression, indicating loss of negative feedback, and reduced WCC expression level, indicating defects in positive feedback. FRH level in *frh*^{R806H} was invariant and similar to WT, suggesting that the mutation affects the protein function but not FRH gene expression or stability.

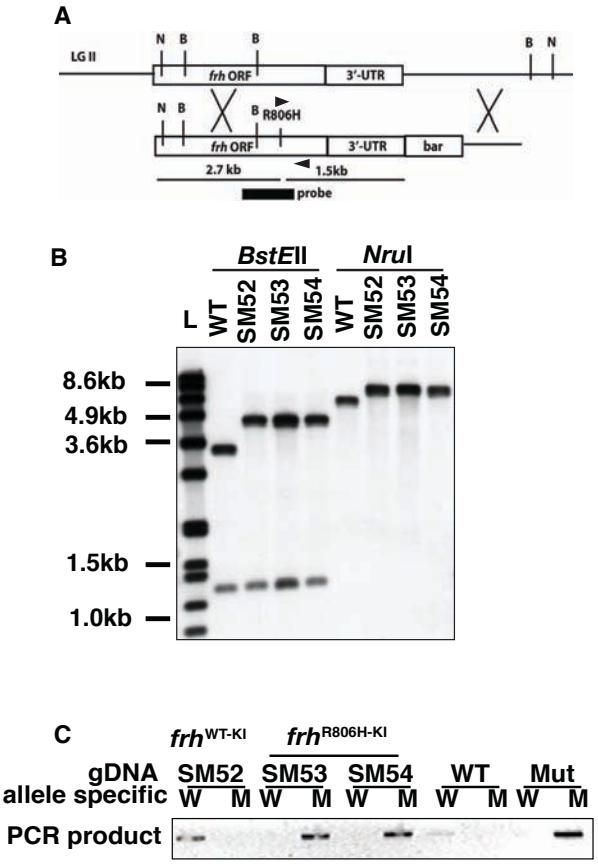

FIGURE S2.—Molecular confirmation and characterization of the *frh*$^{R806H\text{-}KI}$ strains examined in Figure 4. (A) Constructs bearing *frh*^{WT} or *frh*^{R806H} flanked by the selectable *bar* marker at the 3' end were transformed into a *mus-52* (*ku80*) strain chosen to foster a high rate of homologous recombination (COLOT *et al.* 2006; NINOMIYA *et al.* 2004). The thick bar region represents a probe used in the Southern analysis below. The double crossovers point to the approximate positions where the recombination would occur to generate *frh* knock-in strains. Arrow heads mark the positions of PCR primers used in (C). (N: *Nru*I site, B: *Bst*EII site) (B) Genomic DNA samples from WT, *frh*$^{WT\text{-}KI}$ and *frh*$^{R806H\text{-}KI}$ were subjected to enzyme digestion and Southern analysis. Since knock-in strains contained the selectable marker *bar*, a size shift was expected and also observed on the Southern gel confirming the strain identity. (C) A G-A missense mutation was found by sequencing in the *frh*^{R806H} allele. Based on this, allele specific oligos (see materials and methods) were used in PCR analyses to differentiate *frh*$^{R806H\text{-}KI}$ and *frh*$^{WT\text{-}KI}$.

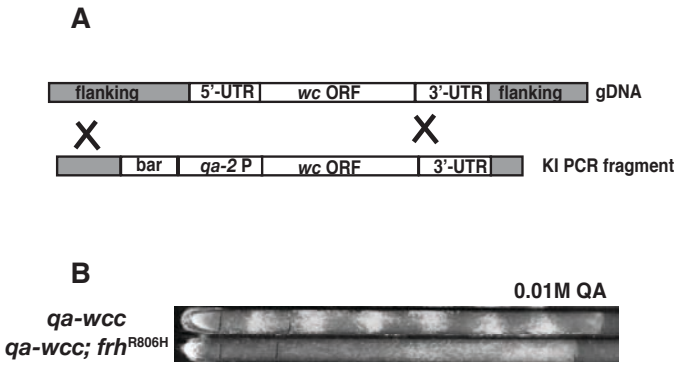

FIGURE S3.—Restoration of positive feedback in *frh*^{R806H}. (A) Diagram of the knock-in strategy used to replace the *wc-1/wc-2* loci with QA inducible *wc-1/wc-2* constructs. *qa-2* P: *qa-2* promoter region. Those two constructs were transformed into *frh*^{R806H} respectively, and a cross between *qa-wc-1; frh*^{R806H} and *qa-wc-2; frh*^{R806H} was made to obtain a *qa-wc-1; qa-wc-2; frh*^{R806H} strain in the progeny. (B) Race tube assay of strains overexpressing WC-1 and WC-2 in *frh*^{R806H}. Restoration of the positive feedback loop was mimicked through WCC induction by QA. However, the strain was still arrhythmic on race tubes, suggesting that loss of negative feedback in *frh*^{R806H} leads to clock malfunction and that restoring the positive feedback loop alone cannot rescue the clock.

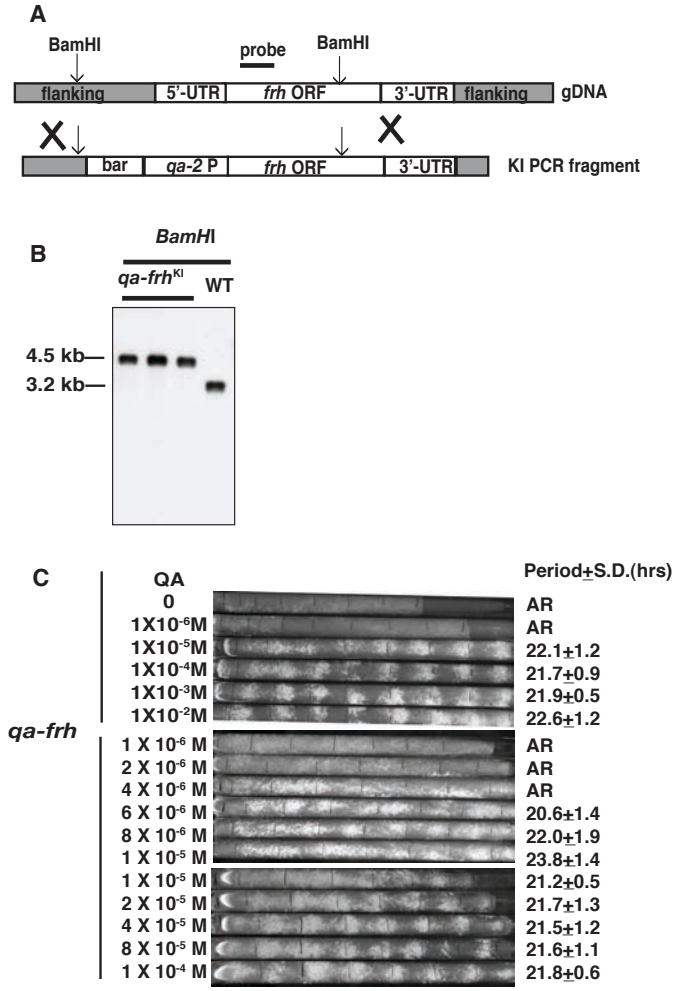

FIGURE S4.—Changing FRH dosage has little or no effect on the circadian clock. (A) Diagram of the knock-in strategy used to replace the *frh* locus with a QA inducible *frh* construct. *qa-2* P: *qa-2* promoter region. Arrowheads point to *Bam*HI sites. (B) Genomic DNA samples digested with *Bam*HI were subjected to Southern analysis using the probe shown in panel A. DNA bands in *qa-frh* strains displayed a size shift due to insertion of *bar* gene in the locus. (C) The *qa-frh* strain was grown on race tubes with different QA concentrations. The strain grew slowly at low QA conditions, consistent with the observation that *frh* is an essential gene (Cheng *et al.* 2005). The rhythm was missing at low QA concentrations, and gradually appeared at QA concentrations around 10^{-5} M. This concentration range was examined more closely in the middle and bottom panels. Around 1×10^{-5} M QA, the strain showed a clock phenotype intermediate between wild type and arrhythmic, suggesting that changes of the FRH level might impact the strength of the negative feedback loop. When the rhythm appeared, however, the period length was wild type, around 22 hours, suggesting that FRH serves as an 'on/off switch' rather than a 'period modulator' in the circadian clock.